

# Gold Nanoparticles: Synthesis, Optical Properties, and Application

V. A. Ogarev\*, V. M. Rudoï, and O. V. Dement'eva

*Institute of Physical Chemistry and Electrochemistry, Russian Academy of Sciences, Moscow, Russia*

\*e-mail: vadim\_ogar@mail.ru

Received April 13, 2017

**Abstract**—The four mostly frequently used gold nanoparticle species—nanospheres, nanorods, nanoshells, and nanocells—whose surface plasmonic resonance peaks lie in the visible to near-infrared range are considered. Their synthesis, optical properties, and some fields of practical application of the relevant materials are analyzed.

**Keywords:** nanoparticles, synthesis, optical properties, gold, biomedicine, surface plasmonic resonance

**DOI:** 10.1134/S2075113318010197

Bulk gold possesses high electrical conductivity, reflectivity, and fluidity, as well as high corrosion and oxidation resistance. Meanwhile, its refinement to nanoscale sizes leads to new interesting properties that expand their range of application. One of most impressive and useful changes arises when gold nanoparticles interact with light. Light illumination of gold nanoparticles causes strong absorption or/and scattering at certain resonance wavelengths that depend to a large extent on their morphology and dielectric medium. Subjected to light irradiation, the conduction electrons in a gold nanostructure are driven by an electric field for collective vibration at a resonant frequency relative to positive ions of the lattice. This phenomenon has been known as localized surface plasmon resonance (LSPR), which underlies many state-of-the-art applications of gold nanoparticles [1]. For example, it was utilized hundreds of years ago to impart a rich red color to the stained-glass windows of churches, but systematic investigation began after Faraday demonstrated the synthesis of colloidal gold in an aqueous medium [2]. The next plunge was taken when Mie [3] solved a Maxwell equation for spherical particles that made it possible to predict and interpret the properties of gold nanoparticles. Their synthesis was reliably and simply pioneered by Turkevich et al. [4]. To date, both approaches have been applied successfully.

When light hits a gold nanoparticle, the free electrons of the metal immediately form an electromagnetic field and begin collective oscillations relative to the lattice of positive ions at a frequency matching that of the incident light. Figure 1 is a schematic of this phenomenon for a gold nanosphere, clarifying the essence of localized surface plasmon resonance.

Surface plasmon resonance (SPR) may occur in any nanomaterial with a high enough density of free

electrons, including metals and heavily doped semiconductors [5, 6]. The process is divided into two types of interaction between the light and the material, which are scattering (the incident light seems to reradiate at the same frequency, but in all directions) and absorption (the light transforms (converts) into heat, or a crystal lattice vibration). Together, these two processes lead to extinction, in other words, to weakening of the incident light intensity (extinction = scattering + absorption). Strong electric fields generated at the nanostructure surface can be used for amplification of the optical signals (e.g., fluorescence and Raman scattering) that arise from the molecules near the surface [5, 6].

The peak position and scattered-to-absorbed light ratio of a gold nanostructure are determined by several parameters, such as size, shape, structure, and morphology, as well as the medium around the nanoparticle surface [5]. The surface plasmon resonance peak of a gold nanoparticle shifts with the change in the dielectric constant of the environment. This phenomenon is used for optical probing.

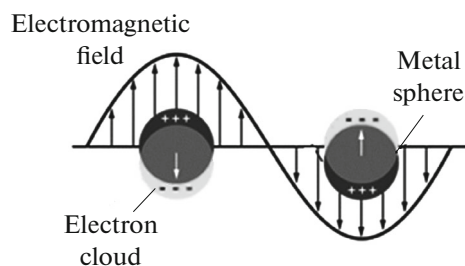


**Fig. 1.** Schematic illustration of collective vibration of the free electrons in a gold nanosphere, which are responsible for surface plasmon resonance.

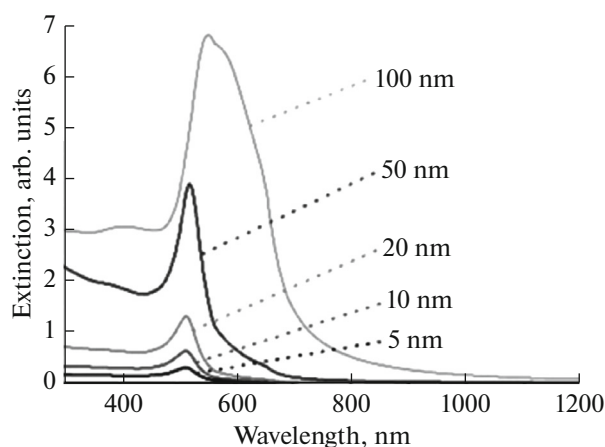


**Fig. 2.** Extinction spectra calculated for gold nanospheres with sizes of 5 to 100 nm in the context of the Mie theory [7].

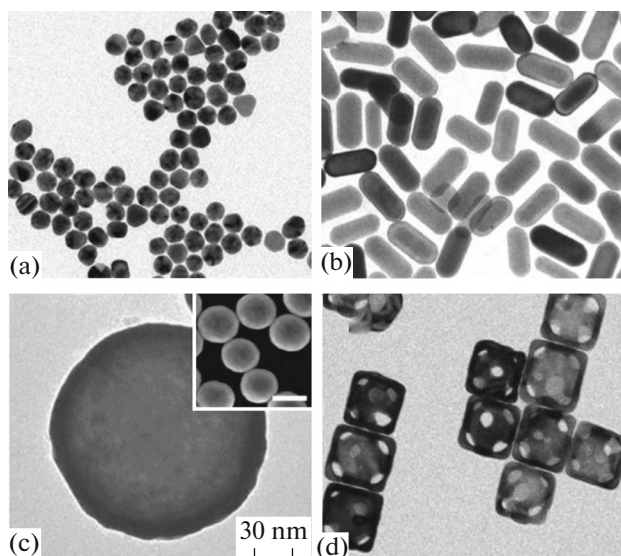


**Fig. 3.** Most common gold nanoparticles: (a) nanospheres; (b) nanorods; (c) nanoshells (silica granules covered with a polycrystal gold layer) (scale in the inset is 200 nm [5]); (d) nanocells.

When the sizes of spherical gold nanoparticles change, the SPR peak position shifts slightly. This is shown in Fig. 2 for the absorption spectra of nanospheres with sizes of 5 to 100 nm [7], which have been calculated in the context of the Mie theory [3]. The SPR peak is at 520 nm. As is obvious, it shifts slightly toward the red region when the particle diameter increases to 100 nm. The spectral broadening is attributed to attenuation of increased radiation for coarse particles. We repeat that the SPR peak position for gold depends on the dielectric constant of the environment. Hence, various solvents and molecules adsorbed on nanospheres may affect the SPR peak position.

Nanoparticle aggregation causes the color changes in suspension from red to violet. This is due to plasmon interfacing between the particles.

In biochemistry, the most attractive are gold nanoparticles with a SPR peak near the infrared region (650–900 nm). In this wave range, the light is capable of easily penetrating deep into soft tissues owing to low absorption by blood and water, as well as to slight dissipation of soft tissue. Therefore, for biomedical purposes, it is essential to rely not on the Au nanoparticle sizes, but on other parameters [6, 8].

Besides unique optical properties of nanoparticles, gold is known as one of the most weather-resistant metals. Even no single-layer gold oxide traces have been detected on the surface exposed to the air. In addition, some works [5, 6] report low toxicity of gold nanomaterials, although there are other data [9].

The stable and bioinert nature of gold nanoparticles makes them excellent candidates for both in situ and in vivo studies of bioprocesses.

There are four morphological species of gold nanostructures that are most extensively used, especially in biomedical applications. They are nanospheres and three types of nanostructures possessing stable surface plasmon resonance in the near-infrared region, which are gold nanorods, nanoshells (silica balls covered with a polycrystal gold layer), and nanocells. The transmission electron microscopy images of all four types of gold nanostructures are shown in Fig. 3.

**Gold nanospheres.** These nanostructures are the simplest species for synthesis and may be obtained with various sizes of highly uniform particles. The nanoparticles prepared in a liquid medium tend to form a spherical shape because of the smallest surface area of the latter relative to species of other shape (at constant volume). However, most of the nanospheres considered in the literature possess an irregular spherical shape; among them, there are many twin particles with a more or less rounded profile. It is thus correct to call them quasi-spherical.

The most common way to achieve spherical gold nanoparticles is based on the reduction of a water-soluble gold salt  $\text{HAuCl}_4$  with a citrate ion (sodium salt of citric acid) [4]. Here, a citrate ion serves also as a reducing agent and anion stabilizer of particles. To date, there are well-established techniques for synthesis of spherical gold nanoparticles of various colors and high uniformity. A ruby red color of suspensions of spherical gold nanoparticles is quantitatively explained by the reflection of electromagnetic waves from nanoparticles. The light reflection theory relative to spherical particles of any sizes proposed by Mie [3] is the most frequently used for description of the optical properties of metal spherical particles. This theory is based on the exact solution of the Maxwell electromagnetic field equations for a plane wave of interaction with a homogeneous sphere of radius  $R$  with the same dielectric constant as for a bulk metal [10]. The

typical spectra for spherical gold nanoparticles with various sizes are given in Fig. 2.

**Nanorods.** Despite the fact that the nanoparticle size and environment are of great importance to achieve a certain optical spectrum, the particle shape exerts more influence on it [11]. So, for gold nanoparticles, the absorption band splits into two parts when the particles are elongated along one axis. The side ratio (SR) is defined as the value of the long axis (length) divided by the value of the short axis (width) of cylindrical or rodlike particles. When the side ratio increases, the separation energy between the resonance parts of two plasmon bands becomes higher. A high-energy absorption band at 520 nm corresponds to the electron oscillations perpendicular to the main (long) axis of the rod and is called transverse plasmon absorption. Another absorption band at lower energy is induced by the free electron vibrations along the long axis of the rod and is known as longitudinal plasmon absorption. A relevant schematic is shown in Fig. 4.

Since the Mie theory has significant limitations on its application, it required some modifications for description of the plasmon properties of nanorods in [11], where the SPR band was predicted to split into two modes owing to the rod orientation relative to the electric field of the incident light, as is seen in Fig. 4. The derived equations can thus be used for calculation of the attenuation spectra at any size ratio [11].

Another method for calculation of SPR spectra is based on the discrete dipole approximation (DDA). This numerical approximation may be applicable to particles of any shape [13].

It is interesting to mention (see Fig. 4) that the longitudinal plasmon band continuously shifts from the visible to near-infrared region when the side ratio of nanorods increases. At the same time, the transverse resonance band exhibits only a slight blue shift.

There are various techniques for synthesis of gold nanorods; among them, the most common are the electrochemical [14] and seeding [15] methods.

Electrochemical synthesis is conducted in a simple two-electrode cell with a gold slab as anode and a platinum cathode. Both electrodes are immersed in an electrolyte solution that contains the mixture of surface active substances of bromide hexadecyltrimethylammonium (BHDTA) and bromide tetradecylammonium (BTDA). BHDTA serves not only as a conventional electrolyte but also as a medium for preventing the nanoparticle growth in the side direction, whereas BTDA acts as inductor of the rod growth. Before electrolysis, a small amount of acetone and cyclohexane is added to the electrolytic solution. Acetone weakens the micellar structure and cyclohexane is necessary for buildup of extended rod-shaped BHDTA micelles. Electrolysis is carried out at a constant current for about 20 min. During the synthesis, the bulk gold metal passes from the anode to the gold complex ions  $\text{AuBr}_4^-$ , which move toward the cathode

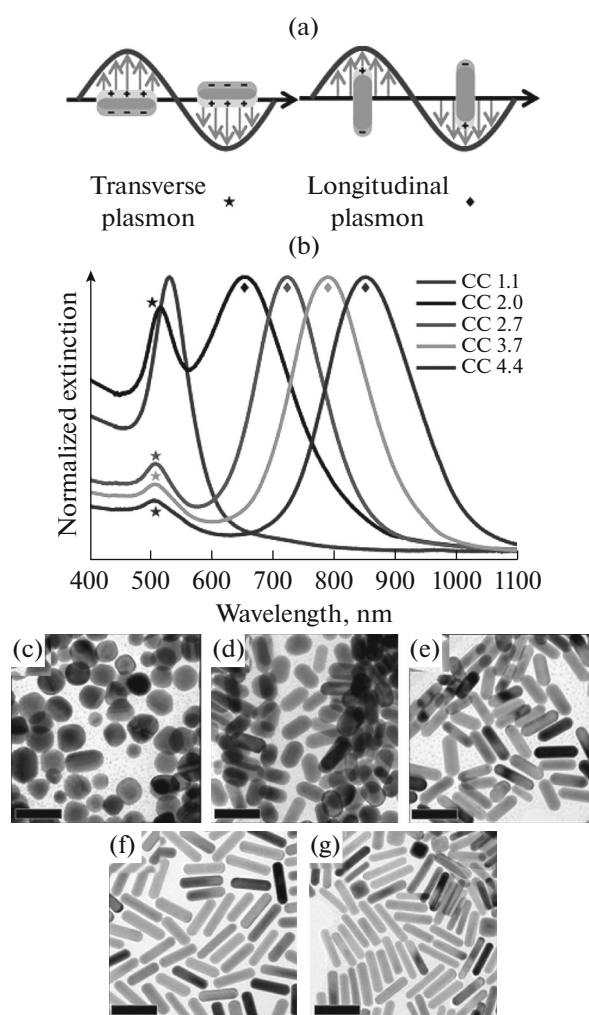


**Fig. 4.** (a) Schematic of a conductive band of oscillating electrons in the transverse and longitudinal directions of surface plasmon resonance of gold nanorods; (b) visible/near-infrared normalized extinction spectrum of gold nanorods with different side ratio (SR). The transverse (\*) and longitudinal (°) extinction peaks are indicated. Tunnel electron microscopy images of gold nanoparticles (scale is 50 nm) with SR: (c) 1.1, (d) 2.0, (e) 2.7, (f) 3.7, and (g) 4.4 correspond to the values of curves in panel (b) from left to right [12].

under the action of the current. There is the reduction reaction at the interface between the cathode and the electrolyte solution. The gold complex ion may also combine with a cation of the surface active substance and favor the formation of rod-shaped gold nanoparticles.

Another way for production of monodispersed gold nanorods is of great interest as well, which is based on a seeding mechanism described in [15]. It involves reducing agents such as hydroxylamine, sodium citrate, and ascorbic acid. The seeding gold particles are initially prepared by reduction of  $\text{HAuCl}_4$  with sodium borohydride ( $\text{NaBH}_4$ ) in the presence of a citrate ion that serves as the surface agent owing to its incapability to reduce the gold salt at room tempera-

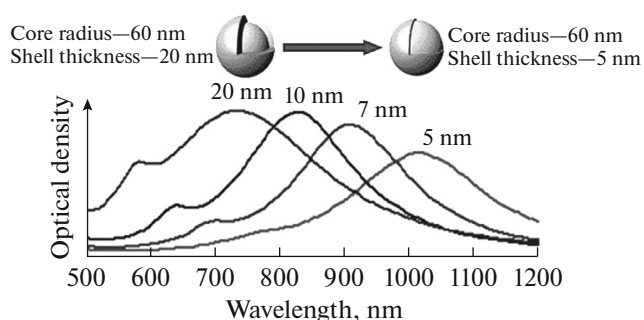


**Fig. 5.** Absorption spectrum of a gold–silicon oxide nanoparticle composite at various core radius–silicon oxide and shell thickness–gold layer ratios [18].

ture. A solution for growth containing  $\text{HAuCl}_4$  with sodium borohydride is mixed with a solution of freshly prepared ascorbic acid (soft reduction) and then added to a seeding solution to obtain gold nanorods.

Although this technique leads to the emergence of nanospheres as well, they can be easily removed by centrifugation with an excess of surface active substances. According to [15], for unexplained reasons at present, the gold nanorods when using seeding nanospheres of  $\sim 3.5\text{--}4.0$  nm are for instance at a maximum  $\sim 20\text{--}30$  nm in width and  $\sim 600$  nm in length. The side ratio parameter (SR) defined as length divided by width varies from  $\sim 2$  to  $\sim 25$  and is controlled by the relative reagent concentrations.

The mechanisms of formation of rod-shaped nanoparticles in a liquid surface active medium were studied in numerous works; some of them were discussed in review [16]. As was assumed, the lead group of a trimethylammonium bromide compound  $\text{C}_{16}\text{TAB}$  can selectively bind to a certain crystallographic face of a seed and/or rods, whereas the tails form a bilayer structure, interacting through the van der Waals forces. These bilayers play an important role in nanorod buildup. According to the experiments, applying surface active compounds with longer chains results in longer rods and their higher yield compared to the short-chain compounds.

It was theoretically shown [17] that composite spherical particles composed of a metal shell and a dielectric core exhibit a significant increase in the SPR mode with the wavelengths tunable over a wide electromagnetic spectral range. As is established in [18], the SPR peaks of these composites—the so-called gold nanoshells—can be easily tuned by controlling the ratio of shell thickness to particle diameter. Figure 5 displays a SPR spectrum of gold nanoparticles calculated via the discrete-dipole approach (DDA). To calculate the core diameter, the silica particle size was fixed at 60 nm, and the shell thickness varied from 5 to 20 nm. As is seen, the plasmon properties of a gold nanoshell are very sensitive to slight changes in the shell thickness—gold layer. The SPR peak shifts from 900 to

1000 nm at a shell thickness variation from 7 to 5 nm, but the dependence of the peak position becomes less sensitive with increased shell thickness.

Gold nanoshells are most frequently synthesized via direct deposition of gold onto spherical colloidal silica particles [18]. First, homogeneous silica spheres are formed, whose surface is subjected to modification with a single-layer of 3-amine-propyltriethoxysilane. After that, colloidal gold with a particle size of 1–2 nm is added to the solution, which reacts with the amino groups of the modifier. A thicker gold layer is deposited onto the surface via chemical reduction. It is worth mentioning that one observes the nonuniform growth of gold grains at some sites upon the above synthesis; i.e., the nanoparticle surface is rough.

**Gold nanocells.** These unique nanostructures can be used in drug delivery. Moreover, hollow internal space of particles can be filled with some small objects to design polyfunctional hybrid nanostructures. The SPR peaks can be tuned with respect to the near-infrared spectrum via control of the wall thickness and porosity.

Gold nanocells can easily be produced using a silver nanocube template through a well-known galvanic substitution reaction in solutions. Silver nanocubes are obtained via a polyol synthesis by reduction of silver nitrate in ethylene glycol in the presence of an inductor (sodium sulfide) and polyvinyl pyrrolidone. The driving force of the displacement reaction is caused by a higher standard potential of the reduction reaction of the  $\text{AuBr}^-/\text{Au}$  pair than for  $\text{Ag}^+/\text{Ag}$ . Figure 6 displays scanning electron and tunnel microscopy images (insets—30 nm). The angular length and thickness of a nanocell wall are  $\sim 36$  and 3.3 nm, respectively, which is close to the values established from the substitution reaction (i.e., oxidation of every three Ag atoms generates a single Au atom). Figure 7a shows the SPR peak shift from the visible to near-infrared region upon transition from silver nanocubes to gold nanocells. Figure 7b demonstrates the extinction, absorption, and scattering spectra of the gold nanoparticles, calculated in the context of the discrete-dipole approach. Gold nanocells can be obtained over a broad range by varying the initial silver nanocube sizes.

Gold nanoparticles are widely used in many applications. Extremely useful for researchers are the results obtained in [20], where the spectra of gold nanoparticles were calculated in the context of the Mie theory [3] and the discrete-dipole approach [13]. The calculations are implemented with respect to absorption and scattering efficiency and to the optical resonance wavelength and generally reveal that the optical properties of nanoparticles depend to a large extent on shape, size, and core/shell composition. For instance, it is clear that gold nanoparticles and nanorods better than others are suitable for studies in a living body, because their optical resonance peak manifests itself in

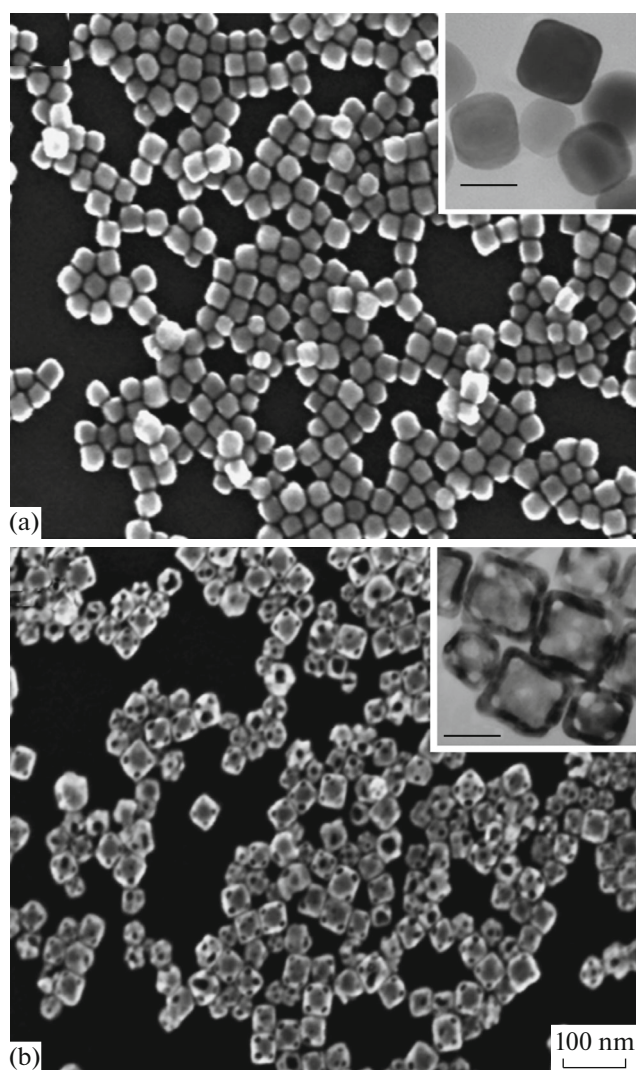


**Fig. 6.** Scanning electron microscopy images of (a) silver nanocubes and (b) gold nanocells. In the right upper corner are the tunnel electron microscopy images; scale is 20 nm [19].

the near-infrared region, which is transparent to body tissues.

Gold nanoparticles possess enhanced absorption and scattering properties that are sometimes five orders in magnitude higher than the extinction coefficients of individual organic dye molecules [21].

Gold nanoparticles attract great attention as colloidal building blocks for microscale optical and electronic devices. They can be made either as self-assembling colloidal blocks or as inkjet printing for templates with good lithographic resolution compared to the manufacture of devices via the top-down traditional methods [22].

Despite the fact that bulk gold is chemically inert, small cluster formations possess catalytic activity, as found in [23]. This is explained by the specific electron structure, shape, and size, as well as the oxidation state

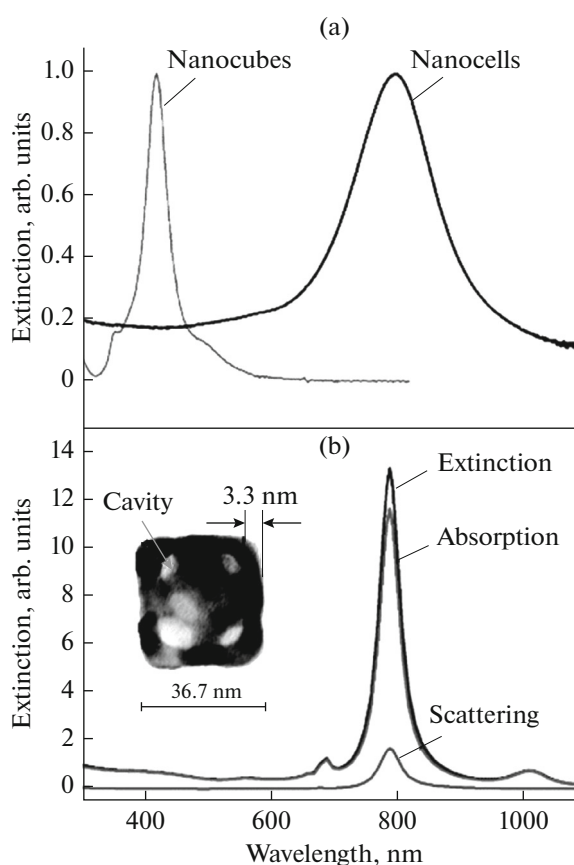


**Fig. 7.** (a) Extinction spectral shift toward the near-infrared region in conversion from silver nanocubes into gold nanocells of the same size; (b) spectra calculated for gold nanocells (inset—gold nanoparticle pictured in a tunnel electron microscope [19]).

of nanoparticles. The surface occupied by nanoclusters may also exert an influence on their catalytic activity. In [24], the authors studied the ability to precipitate gold nanoclusters onto the surface of vitreous polymers, as well as the depth of their immersion and ways of their growth to the desired sizes. These studies allow new functional properties of nanoparticles to be discovered.

The thermal properties of gold nanoparticles under light beams are of particular interest. Compared to other nanometal particles, gold possesses chemical stability. It is also biocompatible in the bulk, and its absorption wavelength may vary from 500 to 1000 nm, depending on the particle shape [21, 25]. Simple inspection of the absorption cross sections of gold, incident light power, and thermal conductivity and heat capacitance of the conventional solvents reveals that illumination in the plasmon range of gold may cause an increase in the temperature of a system by 4–40°C in a steady state. A more pronounced temperature increase near the gold surface at using femtosecond lasers is possible as well [26]. These photothermal effects are able to kill cancer cells or bacteria and can

be used for stimulation of endothermic reactions, because an increase in temperature shifts the reaction equilibrium toward the formation of reaction products [26]. In [27], aggregate-stable dispersed particles with anisotropic core of iron hydroxide with a gold or silver nanoshell, characterized by a plasmon absorption maximum near 1000 nm, i.e., in the transparency range of biological tissues, are examined. The possibility of fine tuning of a SPR position to a given wavelength by means of a controlled change in the metal shell thickness with an extremely small step is demonstrated. Modification of these composite particles with polyethylene glycole (PEG) increases substantially the stability of their aqueous compounds. Quantitative information on distribution of Fe OOH-core/Au-shell/PEG particles was for the first time collected in some organs and tissues of tumor-bearing mice after their intravenous injection as a colloidal solution. As established, composite particles can remain in the blood flow without aggregation and accumulate in a tumor. The *in vivo* studies testify to high efficiency of thermosensitizing action of particles in pulsed laser therapy of tumors.

One of the essential directions is using gold nanoparticles as drug supports [28–30]. This is due to relative biological inertness of nanoparticles and ability to control their distribution in the body by grafting biologically active molecules onto the particle surface or by changing their size or shape. These abilities provide selective accumulation of nanoparticles that carry a specific functional compound in a target organ or tissue. This is of fundamental importance for many drugs, e.g., photosensitizers—compounds capable of inducing formation of singlet oxygen and peroxide radicals under the action of light radiation and used in photodynamic therapy of tumors and other diseases [31]. Many compounds are poorly soluble in water and characterized by low selectivity, which makes their practical application difficult. Grafting photosensitizer molecules on a gold nanoparticle surface could help to solve this problem, but also improve the properties of a drug on account of localized SPR. In [32], there was conducted a synthesis of water-soluble photosensitizer mono[N-(1-carboxymethyl-1-mercaptomethyl) metyl] imide octa-4,5-carboxyphtalocyanine (MOCPC) of zinc and its conjugates with gold nanoparticles with different sizes, and their spectral characteristics were studied. This allowed gathering information on the amount of phtalocyanine molecules drafted to the gold sol nitrate nanoparticles with a diameter of 15 nm. As established, a photosensitizer chemisorbed at the surface of gold nanoparticles exhibits quite intense fluorescence.

Plasmon-enhanced thin films of solar cells are ones of next-generation solar-energy transducers. Thin films of solar elements made of silicon or organic polymers are attractive as lightweight and flexible devices. Plasmon activation with gold nanoparticles was aimed at not only increasing light absorption in

the visible and near-infrared regions but also increasing the coefficient of photon capture inside the device by scattered light. Moreover, huge electric fields generated on the metal surface by plasmon-range illumination improve the capability of neighboring molecules to absorb light themselves. Finally, the presence of electrically conductive nanoparticles in a solar cell could improve the efficiency of the charge carriers reaching the electrodes [33–35].

To conclude, it is worth mentioning the great success in studying metal nanomaterials and their use from cancer tumor therapy to third-generation solar battery cells, but synthesis of the required amount of functional nanocompounds remains a still unsolved task. To date, the material yield achieved by synthesis is usually in milligrams, and the applied method is difficult in large-volume fabrication. Thus, the use of nanomaterials is rapidly expanding, but their synthesis is extensively being studied. Moreover, synthesis of this kind of materials requires an adequate combination of simplicity, reproduction of the properties, and acceptable cost of the product. In [36], this is considered in the case of liquid reactors.

The expansion of the range of application and more efficient use of metal nanoparticles necessitate searching for other routes of nanoparticle surface modification, especially for biomedical purposes [37].

## REFERENCES

1. Eustis, S. and El-Sayed, M.A., Why gold nanoparticles are more precious than pretty gold: noble metal surface plasmon resonance and its enhancement of the radiative and nonradiative properties of nanocrystals of different shapes, *Chem. Soc. Rev.*, 2006, vol. 35, no. 3, pp. 209–217.
2. Faraday, M., The Bakerian Lecture: Experimental relations of gold (and other metals) to light, *Philos. Trans. R. Soc. London*, 1857, vol. 147, pp. 145–181.
3. Mie, G., Beitrage zur Optik truben medien, speziell kolloidaler metallosyngen, *Ann. Phys.*, 1908, vol. 330, no. 3, pp. 377–445.
4. Turkevich, J., Stevenson, P.C., and Hillier, J., A study of the nucleation and growth processes in the synthesis of colloidal gold, *Discuss. Faraday Soc.*, 1951, vol. 11, pp. 55–75.
5. Cogley, C.M., Chen, J., Cho, E.C., Wang, L.V., and Xia, Y., Gold nanostructures: a class of multifunctional materials for biomedical applications, *Chem. Soc. Rev.*, 2011, vol. 40, no. 1, pp. 44–56.
6. Dreaden, E.C., Alkilany, A.M., Huang, X., Murphy, C.J., and El-Sayed, M.A., The gold age: gold nanoparticles for biomedicine, *Chem. Soc. Rev.*, 2012, vol. 41, no. 7, pp. 2740–2779.
7. Hu, M., Chen, J., Li, Z.-Y., Au, L., Hartland, G.V., Li, X., Marquez, M., and Xia, Y., Gold nanostructures: engineering their plasmonic properties for biomedical applications, *Chem. Soc. Rev.*, 2006, vol. 35, no. 11, pp. 1084–1094.
8. Huang, X., Neretina, S., and El-Sayed, M.A., Gold nanoroads: from synthesis and properties to biological

- and biomedical applications, *Adv. Mater.*, 2009, vol. 21, pp. 4880–4910.
9. Khlebtsov, N. and Dykman, L., Biodistribution and toxicity of engineered gold nanoparticles: a review of in vitro and in vivo studies, *Chem. Soc. Rev.*, 2011, vol. 40, no. 3, pp. 1647–1671.
  10. Ghosh, S.K. and Pal, T., Interactive coupling effect on the surface plasmon resonance of gold nanoparticles: from theory to application, *Chem. Rev.*, 2007, vol. 107, no. 11, pp. 4797–4862.
  11. Link, S. and El-Sayed, M.A., Shape and size dependence of radioactive, non-radioactive and photothermal properties of gold nanocrystals, *Int. Rev. Phys. Chem.*, 2000, vol. 19, no. 3, pp. 409–453.
  12. Abadeert, N.S., Brennan, M.R., Wilson, W.L., and Murphy, C.L., Distance and plasmon wavelength dependent fluorescence of molecules bond to silica-coated gold nanorods, *ACS Nano*, 2014, vol. 8, no. 8, pp. 8392–8406.
  13. Kelly, K.L., Coronado, E., Zhao, L.L., and Schatz, G.C., The optical properties of metal nanoparticles: the influence of size, shape, and dielectric, *J. Phys. Chem. B*, 2003, vol. 107, no. 3, pp. 668–677.
  14. Chang, S.-S., Shih, Ch.-W., Chen, Ch.-D., Lai, W.-Ch., and Chris-Wang, C.R., The shape transition of gold nanorods, *Langmuir*, 1999, vol. 15, no. 3, pp. 701–709.
  15. Murphy, C.J., Sau, T.K., Gole, A.M., Orendorff, Ch.J., Gao, J., Gou, L., Hunyadi, S.E., and Li, T., Anisotropic metal nanoparticles: synthesis, assembly and optical applications, *J. Phys. Chem. B*, 2005, vol. 109, no. 29, pp. 13857–13870.
  16. Perez-Juste, J., Pastoriza-Santos, I., Liz-Marzan, L.M., and Mulvaney, P., Gold nanorods: synthesis, characterization and application, *Coord. Chem. Rev.*, 2005, vol. 249, nos. 17–18, pp. 1870–1901.
  17. Neeves, A.E. and Birnboim, M.H., Composite structures for the enhancement of nonlinear optical susceptibility, *J. Opt. Soc. Am. B*, 1989, vol. 6, no. 4, pp. 787–796.
  18. Oldenburg, S.J., Averitt, R.D., Westcott, S.L., and Halas, N.J., Nanoengineering of optical resonances, *Chem. Phys. Lett.*, 1998, vol. 288, nos. 2–4, pp. 243–247.
  19. Chen, J., Saeki, F., Wiley, B.J., Cang, H., Cobb, M.J., Li, Z.-Y., Au, L., Zhang, H., Kimmey, M.B., and Xia, Y.L., Gold nanocages: bioconjugation and their potential use as optical imaging contrast agents, *Nano Lett.*, 2005, vol. 5, no. 3, pp. 473–477.
  20. Jain, P.K., Lee, K.S., El-Sayed, I.H., and El-Sayed, M.A., Calculated absorption and scattering properties of gold nanoparticles of different size, shape, and composition: application in biological imaging and biomedicine, *J. Phys. Chem. B*, 2006, vol. 110, no. 14, pp. 7238–7248.
  21. Eustis, S. and El-Sayed, M.A., Why gold nanoparticles are more precious than pretty gold: nobelmetal surface plasmon resonance and its enhancement of the radiative and nonradiative properties of nanocrystals of different shapes, *Chem. Soc. Rev.*, 2006, vol. 35, no. 3, pp. 209–217.
  22. Cutler, J.I., Auyeung, E., and Mirkin, Ch.A., Spherical nucleic acids, *J. Am. Chem. Soc.*, 2012, vol. 134, no. 3, pp. 1376–1391.
  23. Chen, M.S. and Goodman, D.W., The structure of catalytically active gold on titania, *Science*, 2004, vol. 306, no. 5694, pp. 252–255.
  24. Dement'eva, O.V., Kartseva, M.E., Ogarev, V.A., Sukhov, V.M., and Rudoy, V.M., Metal nanoparticles on polymer surfaces. 7. The growth kinetics of gold nanoparticles embedded into surface layers of glassy polymers, *Colloid J.*, 2017, vol. 79, no. 1, pp. 42–49.
  25. Alkilany, A.M., Thompson, L.B., Boulos, S.P., Sisco, P.N., and Murphy, C.J., Gold nanorods: their potential for photothermal therapeutics and drug delivery, tempered by complexity of their biological interactions, *Adv. Drug Delivery Rev.*, 2012, vol. 64, no. 2, pp. 190–199.
  26. Lal, S., Clare, S.F., and Holas, N.J., Nanoshell-enabled photothermal cancer therapy: impending clinical impact, *Acc. Chem. Res.*, 2008, vol. 41, no. 12, pp. 1842–1851.
  27. Huang, J., Jackson, K.S., and Murphy, C.J., Polyelectrolyte wrapping layers control rates of photothermal molecular release from gold nanorods, *Nano Lett.*, 2012, vol. 12, no. 6, pp. 2982–2987.
  28. Dement'eva, O.V., Filippenko, M.A., Kartseva, M.E., Sedykh, E.M., Bannykh, L.N., Yakubovskaya, R.I., Pankratov, A.A., Kogan, B.Ya., and Rudoy, V.M., Synthesis of anisotropic plasmonic nanoparticles with core-shell structure and prospects of their application in laser treatment of tumors, *Nanotechnol. Russ.*, 2012, vol. 7, nos. 9–10, pp. 517–526.
  29. Llevot, A. and Astruc, D., Applications of vectorized gold nanoparticles to the diagnosis and therapy of cancer, *Chem. Soc. Rev.*, 2012, vol. 41, no. 1, pp. 242–257.
  30. *Gold Nanoparticles for Physics, Chemistry and Biology*, Louis, C. and Pluchery, O., Eds., London: Imperial Coll. Press, 2012.
  31. Vigderman, L. and Zubarev, E.R., Therapeutic platforms based on gold nanoparticles and their covalent conjugates with drug molecules, *Adv. Drug Delivery Rev.*, 2013, vol. 65, no. 5, pp. 663–676.
  32. Celli, J.P., Spring, B.Q., Rizvi, I., Evans, C.L., Samkoe, K.S., Verma, S., Pogue, B.W., and Hasan, T., Imaging and photodynamic therapy: mechanisms, monitoring, and optimization, *Chem. Rev.*, 2010, vol. 110, no. 5, pp. 2795–2838.
  33. Dement'eva, O.V., Vinogradova, M.M., Luk'yanets, E.A., Solov'eva, L.I., Ogarev, V.A., and Rudoy, V.M., Zinc phthalocyanine-based water-soluble thiolated photosensitizer and its conjugates with gold nanoparticles: synthesis and spectral properties, *Colloid J.*, 2014, vol. 76, no. 5, pp. 539–545.
  34. Ferry, V.E., Verschunren, M.A., Li, H.B., Verhagen, E., Walters, R.J., Schropp, R.E., Atwater, H.A., and Polman, A., Light trapping in ultrathin plasmonic solar cells, *Opt. Express*, 2010, vol. 18, no. 13, pp. A237–A245.
  35. Ferry, V.E., Polman, A., and Atwater, H.A., Modeling light trapping in nanostructured solar cells, *ACS Nano*, 2011, vol. 5, no. 12, pp. 10055–10064.
  36. Ogaryov, V.A., Rudoy, V.M., and Dementyeva, O.V., Metal nanoparticles and quantum dots as photosensitizers of solar cell batteries, *Inorg. Mater.: Appl. Res.*, 2016, vol. 7, no. 4, pp. 509–516.
  37. Song, Y., Hormes, J., and Kumar, C.S., Microfluidic synthesis of nanomaterials, *Small*, 2008, vol. 4, no. 6, pp. 698–711.
  38. Verma, A. and Stellacci, F., Effect of surface properties on nanoparticle-cell interactions, *Small*, 2010, vol. 6, no. 1, pp. 12–21.

Translated by O. Maslova